

# Radio, optical and X-ray nuclei in nearby 3CRR radio galaxies

M.J. Hardcastle and D.M. Worrall

*Department of Physics, University of Bristol, Tyndall Avenue, Bristol BS8 1TL*

11 June 2021

## ABSTRACT

*HST* observations have shown that low-redshift 3CR radio galaxies often exhibit a point-like optical component positionally coincident with the GHz-frequency radio core. In this paper we discuss the correlation between the luminosities of the radio, optical and X-ray cores in these objects, and argue that all three components have a common origin at the base of the relativistic jets. In unified models, FRI radio galaxies should appear as dimmed, redshifted versions of BL Lac objects. We show that such models are consistent with the spectral energy distributions of the radio galaxies only if the nuclear X-ray emission in radio galaxies is inverse-Compton in origin.

**Key words:** galaxies: active – galaxies: nuclei – BL Lacertae objects: general – X-rays: galaxies

## 1 INTRODUCTION

On sub-arcsecond scales, the central radio components, or ‘cores’, of radio galaxies are understood, as a result of VLBI observations, to be the unresolved bases of the relativistic jets that transport energy to the lobes, seen in partly self-absorbed synchrotron radiation. Superluminal motion is seen in some sources, and the supposed unification of radio galaxies with BL Lac objects and quasars (e.g. Urry & Padovani 1995) requires the cores to be relativistically beamed with Lorentz factors  $\gtrsim 5$ . Hardcastle & Worrall (1999) and Canosa et al. (1999) have found that the nuclear soft-X-ray emission in radio galaxies is well correlated with the core radio emission. This finding implies that the X-ray emission is also relativistically beamed and so must originate in the jet, and is qualitatively consistent with models in which the strong X-ray emission of BL Lac objects is largely a result of relativistic boosting.

A snapshot survey of 3CR radio sources with the *HST* Wide Field and Planetary Camera 2 (WFPC2) (De Koff et al. 1996) has detected unresolved optical nuclear components in a large number of objects, particularly at low redshift (Martel et al. 1999), where, because of the luminosity-redshift correlation in the 3CR sample, most radio sources are of type FRI rather than FRII (Fanaroff & Riley 1974). Chiaberge, Capetti & Celotti (1999) find that the optical luminosities of the FRI radio galaxies are correlated with the luminosities of their 5-GHz radio cores, which, by the same argument as used by Hardcastle & Worrall for the X-ray emission, implies a jet-related origin for the nuclear optical emission. Capetti & Celotti (1999) compare the optical nu-

clear luminosities of five of the detected FRI radio galaxies with those of BL Lac objects matched in isotropic properties and find support for unification in the optical assuming relativistic jets with Lorentz factors in the range 5 to 10. In this paper we examine the radio, optical and X-ray nuclear fluxes and luminosities of a sample of low-redshift radio galaxies in order to explore the X-ray and optical emission mechanisms.

Throughout the paper we adopt a cosmology with  $H_0 = 50 \text{ km s}^{-1} \text{ Mpc}^{-1}$ . Spectral index  $\alpha$  is defined in the sense that flux density is proportional to  $\nu^{-\alpha}$ .

## 2 OBSERVATIONS AND DATA REDUCTION

We selected the 27 radio galaxies with  $z < 0.06$  from the 3CRR sample (Laing, Riley & Longair 1983, Laing & Riley, in prep.); the redshift limit was chosen to ensure good spatial resolution, so that nuclei could adequately be separated from the dusty discs that surround them. The status of the archival WFPC2 *HST* observations of these objects is tabulated in Table 1. The majority of the observations were made as part of the snapshot survey, and so are short (280 s) and use the Planetary Camera (PC) with the F702W filter, but we have used longer observations in this or other broad-band red filters where they exist in the archives. Bias subtraction and flat-field corrections had been applied automatically as part of the standard pipeline, and we performed cosmic ray rejection using the CRREJ program in IRAF.

Almost every observed source (17/20) in this sample has an optical nucleus which is unresolved with the *HST* (i.e.,

has a linear size less than  $\sim 50$  pc), and the majority (13) of these also show disc-like dust features. The two broad-line objects in the sample, 3C 382 and 3C 390.3, show atypically strong nuclei, as would be expected from their ground-based classification as N-galaxies.

For the 17 sources with detected point-like nuclei we used IRAF to carry out small-aperture photometry on the nucleus. Source regions were typically only 3–5 PC pixels (1 pixel is 46 milliarcsec), and backgrounds were taken from an annulus around the source close to the nucleus (up to 10 pixels) to minimise the contribution from the stellar continuum to the net core emission. The resulting measurements were corrected for flux lying outside the extraction regions using the aperture corrections given by Holtzman et al. (1995), and then converted to flux densities at the central frequency of the filter ( $4.3 \times 10^{14}$  Hz for F702W,  $3.8 \times 10^{14}$  Hz for F791W and F814W) using the SYNPHOT package in IRAF, assuming a power-law spectrum with  $\alpha = 0.8$  (the results are insensitive to the assumed spectrum). Flux densities are tabulated in Table 2, together with corresponding radio and X-ray values.

Our analysis is independent of that of Chiaberge et al. (1999), though their sample contains a large number of objects (12 out of the 17 in Table 2) in common with ours. Comparing the flux densities tabulated in their table 3 with our measurements for the overlapping objects, we find agreement to better than a factor of 2 in almost all cases, which is reasonable considering the uncertainties in background subtraction.

### 3 RESULTS

#### 3.1 Radio-optical correlation

The 5-GHz radio versus optical correlation for the 17 sources with point-like optical cores is shown in Fig. 1. The correlation is strong over several orders of magnitude of luminosity, extending further than that of Chiaberge et al. (1999) primarily because of the inclusion of the luminous broad-line objects 3C 382 and 3C 390.3. The optical and radio flux densities are also well correlated, and a partial Kendall's  $\tau$  test shows that the luminosity-luminosity correlation is not induced by a common correlation with redshift (at the 95 per cent confidence level).

The one narrow-line FRII in the sample, 3C 192, lies some way off the correlation. This may be an artefact of the lower resolution of the *HST* observations (Table 1), or it may indicate a difference between FRIs and FRIIs.

All three objects which do not have a measured point-like optical nucleus in the *HST* observations do not have a nucleus for reasons which are likely to be unrelated to their true optical nuclear flux (see notes to Table 1). The sub-sample of 17 sources that we consider is therefore not biased with respect to the optical flux, and the three missing objects would not be expected to alter the correlation of Fig. 1.

#### 3.2 Optical-X-ray correlation

The 17 sources with point-like optical cores were all targets for *ROSAT* pointed observations, and X-ray flux densities

for the cores (almost all of which were detected) are given by Hardcastle & Worrall (1999) and tabulated in Table 2. The X-ray versus radio correlation (Fig. 2) is at least as good as that seen in the radio-optical plot (Fig. 1), and the scatter about a regression line appears to be considerably less, suggesting that there may be a closer relationship between the X-ray and optical emission. Again, 3C 192 is an outlier.

#### 3.3 Colour-colour plots

Rest-frame radio-to-optical and optical-to-X-ray spectral indices ( $\alpha_{RO}$  and  $\alpha_{OX}$ , respectively) are given in Table 2 and plotted in Fig. 3. Also plotted for comparison are the corresponding spectral indices for the X-ray-observed BL Lac objects with measured redshifts in the sample of Fossati et al. (1998). K-corrections were made to all the data points using  $\alpha_R = 0$ ,  $\alpha_O = 0.8$  and  $\alpha_X = 0.8$ , and the BL Lac optical fluxes are also ‘corrected’ from the V-band measurements tabulated by Fossati et al. to our observing wavelength of  $\sim 7000$  Å.

We might expect from unified models that the cores of the FRI radio galaxies would occupy a similar region of the  $\alpha_{RO} - \alpha_{OX}$  plane to radio-selected BL Lac objects (RBLs). In fact, Fig. 3 shows that they occupy a region which overlaps with the RBLs, and is clearly distinguishable from the region occupied by X-ray selected BL Lacs (XBLs); the only two objects to overlap with the XBLs are the broad-line radio galaxies 3C 382 and 3C 390.3. However, there is a clearly distinguishable difference between the radio galaxies and RBLs, in the sense that radio galaxies tend to have steeper  $\alpha_{RO}$  and flatter  $\alpha_{OX}$  than RBLs. Since the distribution of  $\alpha_{RX}$  of FRI radio galaxies, both in this sample and in 3CRR as a whole (Hardcastle & Worrall 1999), is very similar to that of RBLs, this result at first sight implies that radio galaxies tend to have fainter optical cores than we would expect from the behaviour of BL Lacs. We return to this point below.

## 4 DISCUSSION

#### 4.1 FRII objects

The only narrow-line FRII object in the sample is 3C 192, which is an outlier on all the correlations involving optical data, since its optical flux is over-bright relative to its radio or X-ray flux density. There is likely to be a significant amount of line contamination in the *HST* flux of this object, and it was observed with the WFC rather than the PC, reducing our ability to remove background emission. Nevertheless, it is possible that the anomalous behaviour of 3C 192 is an indication of a difference between FRI and FRII objects. No such difference is apparent in the X-ray and radio data alone (Hardcastle & Worrall 1999).

The two broad-line objects, also FRIIs, have colours which are significantly different from those of the rest of the sample. Both objects are affected by saturation of the PC CCDs, but this effect means that we are underestimating the optical fluxes, and they may be even more extreme outliers on Fig. 3. However, both objects are known to be variable in the radio and X-ray, and the data we have used are of varying

vintage, so it is dangerous to draw conclusions concerning broad-line FR II galaxies based on Fig. 3.

#### 4.2 The origins of the optical and X-ray emission

The correlation in Fig. 1 implies that the optical emission originates in the jet. The most likely emission mechanism is then synchrotron radiation, particularly as optical synchrotron emission is seen from the kiloparsec-scale jets of several radio galaxies (e.g. Martel et al. 1998 and references therein), including 3C 66B, 3C 264 and M87 in our sample.

Several factors make it difficult to constrain the process responsible for the X-radiation using the radio and optical emission. We know from the flat radio spectra of the cores that they are self-absorbed at cm wavelengths, so we can draw no strong conclusions on the origins of the optical and X-ray emission from the generally convex shapes of the radio-optical-X-ray spectra; there are few observations of cores of radio galaxies at radio frequencies high enough to avoid self-absorption.

A well-determined core optical spectrum could provide strong clues about the mechanism of the X-rays emission. A second optical colour, in the F547M or F555W filters, is available for a few nuclei in our sample, and in the majority of cases the derived optical spectral index is steeper than the optical-to-X-ray spectral index, which would naïvely suggest that the X-ray and optical emission cannot both be synchrotron emission from a single population of electrons. However, even modest amounts of intrinsic or Galactic reddening can make a substantial difference to the measured optical spectral index (e.g. Ho 1999). Reddening will be significant if the geometry is such that part of a dusty disc lies along the line of sight to the nucleus. In the case of NGC 6251, Ferrarese & Ford (1999) have shown that the reddening inferred from a comparison of the obscured and unobscured regions of the galaxy is consistent with the intrinsic  $N_H$  inferred from X-ray absorption by Birkinshaw & Worrall (1993), so that the dusty disc may be obscuring both the optical and X-ray nuclear emission. 3C 264, where the plane of the disc appears to be almost perpendicular to the line of sight, has the flattest measured optical spectral index in the sample, and so may be the least affected by reddening, consistent with this picture.

Therefore the present data cannot rule out a synchrotron origin for the X-ray emission, when the possible effects of intrinsic reddening are taken into account. If the X-ray cores were synchrotron, it would go some way towards explaining the tight relationship between the optical and X-ray nuclear luminosities. However, an inverse-Compton origin for the X-ray nuclei may be required by unified models, as discussed in the next section. Further *HST* observations are needed to measure the reddening and the intrinsic optical spectral index in a large sample of radio galaxies, if broad-band spectra are to constrain the X-ray emission process.

#### 4.3 Constraints from unified models

We can combine the X-ray, optical and radio data for FRI radio galaxies to provide a new test of the standard BL-Lac/FRI unified model, in which relativistic beaming is important in the nuclei and BL Lac objects are FRIs seen at

small angles to the line of sight. In a such model, the spectral energy distributions (SEDs) of FRIs should be dimmed, redshifted versions of those of RBLs. We can test this model by investigating the regions that the two populations occupy in the  $\alpha_{RO} - \alpha_{OX}$  plane of Fig. 3.

If BL Lac spectra were one-component power laws extending from the radio to the X-ray, we would expect that the FRIs and BL Lacs would populate similar regions of the  $\alpha_{RO} - \alpha_{OX}$  plane. In fact, the SEDs of BL Lac objects between radio and X-ray bands are often well modelled by a smoothly curved function (e.g. a parabola; Landau et al. 1986, Sambruna et al. 1996). Redshifting and dimming such a spectrum to produce the expected spectrum of an FRI radio galaxy should result in both  $\alpha_{RO}$  and  $\alpha_{OX}$  being somewhat steeper in radio galaxies than in RBLs, which is not observed. Instead,  $\alpha_{OX}$  is flatter in radio galaxies. (The effect on the SED from cosmological redshift, given that the RBLs of Fig. 3 are more distant than our sample of FRIs, is small compared to that expected from relativistic beaming.)

The nuclear X-ray emission from the FRIs has been separated from the thermal emission from their host groups or clusters (Hardcastle & Worrall 1999), and we are confident that we are not overestimating the nuclear X-ray emission significantly in these sources. In contrast, the discrepancy between the  $\alpha_{OX}$  distributions for FRIs and BL Lac objects may be underestimated as a result of a thermal contribution to the X-ray fluxes of the RBLs, which can be significant at the  $\sim 10$  per cent level (e.g. Hardcastle, Worrall & Birkinshaw 1999).

Reddening in the optical nuclei observed with *HST*, as a result of absorption by the dusty disc seen in the *HST* images, may have an effect. The FRIs can be made to have a very similar distribution of  $\alpha_{RO}$  to the RBLs if it is assumed that obscuration causes us to underestimate the red optical fluxes by a factor  $\sim 2$  to 3 in the radio galaxies only. However, such a high degree of reddening would imply a typical  $A_V \sim 2$ , and therefore, for typical gas/dust ratios, an intrinsic column density of order  $5 \times 10^{21} \text{ cm}^{-2}$ . Such column densities are somewhat higher than is observed for the soft X-ray cores of well-studied FRIs (e.g. Birkinshaw & Worrall 1993; Worrall & Birkinshaw 1994). More importantly, they would mean that we are underestimating the unabsorbed 1-keV X-ray flux densities of the FRIs (which are calculated on the assumption of galactic absorption) by a similar factor. Thus  $\alpha_{OX}$  is not strongly affected by reddening at this level, and we cannot account for the flat  $\alpha_{OX}$  in radio galaxies in this way.

So the relatively flat  $\alpha_{OX}$  in FRIs appears to be real. If unified models are correct, this observation gives us a strong reason to believe that the X-ray nuclei of FRIs are dominated by inverse-Compton emission. To make the data consistent with unified models, it must be the case that the  $\alpha_{OX}$  of FRIs is observed to be relatively flat because a new component of the RBL spectrum, not well modelled by the simple parabolae of Landau et al. (1986), is dominant at X-ray energies in the FRIs but largely blueshifted out of the observed band in RBLs. In BL Lacs, an inverse-Compton component of the emission has long been expected to dominate at high energies, and this component is believed to be responsible for the second peak in the SED seen in  $\gamma$ -rays at MeV–GeV energies (e.g. Fosatti et al. 1998); discrepancies between the simple parabolic models and the data, and the

flat spectra seen in the X-ray in some BL Lacs, can also be attributed to this component (Worrall 1989; Sambruna et al. 1996).

We therefore favour an inverse-Compton model for the nuclear X-ray emission seen in these nearby radio galaxies. If the X-ray nuclei of FRIs are indeed dominated by inverse-Compton emission, then we expect them to have flat soft X-ray spectra, a prediction that will be testable with forthcoming *Chandra* observations.

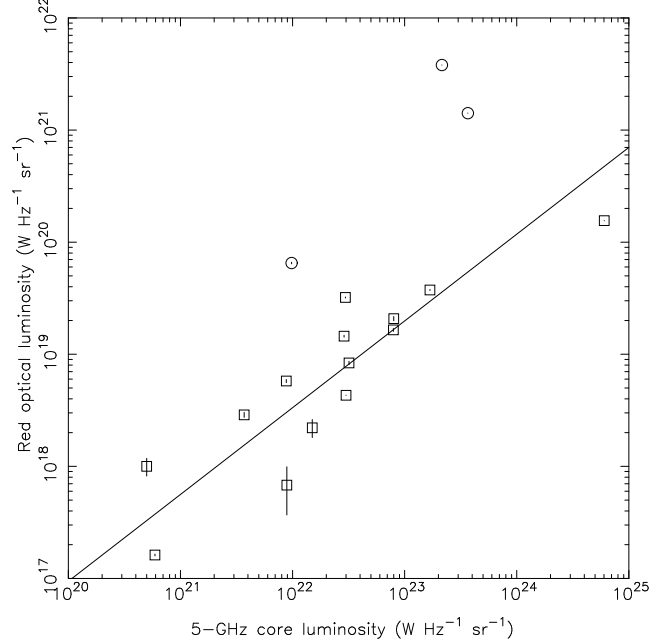
## REFERENCES

- Birkinshaw M., Worrall D.M., 1993, *ApJ*, 412, 568  
 Canosa C.M., Worrall D.M., Hardcastle M.J., Birkinshaw M., 1999, *MNRAS*, 310, 30  
 Capetti A., Celotti A., 1999, *MNRAS*, 304, 434  
 Chiaberge M., Capetti A., Celotti A., 1999, *A&A*, 349, 77  
 De Koff S., Baum S.A., Sparks W.B., Biretta J., Golombek D., Machetto F., McCarthy P., Miley G.K., 1996, *ApJS*, 107, 621  
 Fanaroff B.L., Riley J.M., 1974, *MNRAS*, 167, 31P  
 Ferrarese L., Ford H.C., 1999, *ApJ*, 515, 583  
 Fossati G., Maraschi L., Celotti A., Comastri A., Ghisellini G., 1998, *MNRAS*, 299, 433  
 Gavazzi G., Perola G.C., Jaffe W., 1981, *A&A*, 103, 35  
 Giovannini G., Feretti L., Gregorini L., Parma P., 1988, *A&A*, 199, 73  
 Hardcastle M.J., Worrall D.M., Birkinshaw M., 1999, *MNRAS*, 305, 246  
 Hardcastle M.J., Worrall D.M., 1999, *MNRAS*, 309, 696  
 Holtzman J., et al., 1995, *PASP*, 107, 156  
 Ho L.C., 1999, *ApJ*, 516, 672  
 Jackson N., Sparks W.B., Miley G.K., Macchetto F., 1995, *A&A*, 296, 339  
 Jones D.L., Unwin S.C., Readhead A.C.S., Sargent W.L., Seelstad G.A., Simon R.S., Walker R.C., Benson J.M., Perley R.A., Bridle A.H., Pauliny-Toth I.I.K., Romney J., Witzel A., Wilkinson P.N., B  ath L.B., Booth R.S., Fort D.N., Galt J.A., Mutel R.L., Linfield R.P., 1986, *ApJ*, 305, 684  
 Laing R.A., Riley J.M., Longair M.S., 1983, *MNRAS*, 204, 151  
 Leahy J.P., J  gers W.J., Pooley G.G., 1986, *A&A*, 156, 234  
 Lynds R., 1971, *ApJ*, 168, 87  
 Martel A.R., Sparks W.B., Macchetto D., Biretta J.A., Baum S.A., Golombek D., McCarthy P.J., De Koff S., Miley G.K., 1998, *ApJ*, 496, 203  
 Martel A.R., Baum S.A., Sparks W.B., Wyckoff E., Biretta J.A., Golombek D., Macchetto F.D., De Koff S., McCarthy P.J., Miley G.K., 1999, *ApJS*, 122, 81  
 Noordam J.E., de Bruyn A.G., 1982, *Nat*, 299, 597  
 O’Dea C.P., Owen F.N., 1985, *AJ*, 90, 927  
 Sambruna R.M., Maraschi L., Urry C.M., 1996, *ApJ*, 463, 444  
 Urry C.M., Padovani P., 1995, *PASP*, 107, 803  
 Worrall D.M., 1989, in Maraschi L., Maccacaro T., Ulrich M.-H., eds, *BL Lac objects*, Springer-Verlag, Heidelberg, p. 305  
 Worrall D.M., Birkinshaw M., 1994, *ApJ*, 427, 134

## ACKNOWLEDGEMENTS

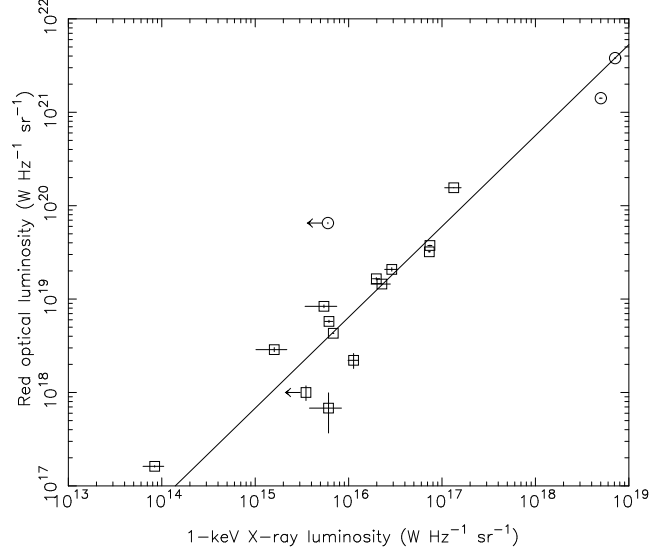
This work was supported by PPARC grant GR/K98582.

**Figure 1.** The radio-optical luminosity-luminosity correlation for  $z < 0.06$  3CRR sources



Squares indicate FRI objects, circles are FRIIs. The two FRIIs at the top right of the plot are the broad-line objects 3C 382 and 3C 390.3, and the other is 3C 192. The FRI to the far right is 3C 84. The optical fluxes of the brightest objects (3C 84, 3C 382 and 3C 390.3) are affected by saturation of the *HST* CCDs, and they are all known to be variable in the radio and X-ray, rendering their positions the most uncertain. The solid line shows the results of a least-squares linear regression on the data for 14 FRI sources.

**Figure 2.** The X-ray-optical luminosity-luminosity correlation for  $z < 0.06$  3CRR sources

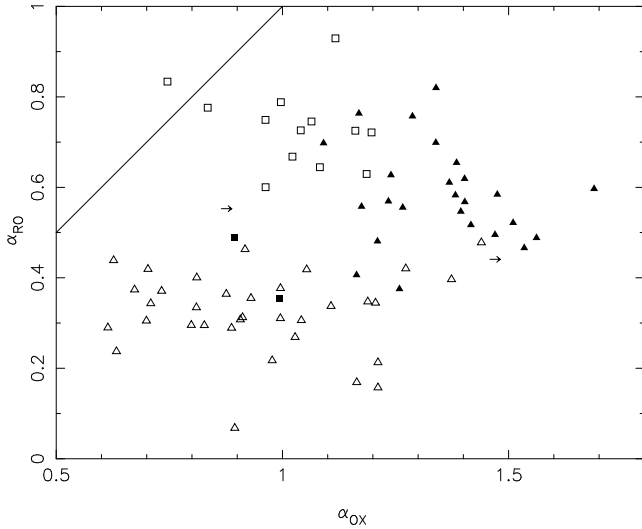


Symbols and notes as for Fig. 1.

**Table 2.** Radio, optical and X-ray flux densities and spectral indices for the objects with detected point-like optical nuclei

Source	$z$	Flux densities at			Ref. for radio	Spectral indices	
		5 GHz (mJy)	Optical ( $\mu$ Jy)	1 keV (nJy)		$\alpha_{\text{RO}}$	$\alpha_{\text{OX}}$
3C 31	0.0167	92	$60 \pm 2$	$64 \pm 7$	1	0.64	1.08
3C 66B	0.0215	182	$90 \pm 2$	$140 \pm 30$	2	0.67	1.02
3C 83.1B	0.0255	40	$3 \pm 1$	$30 \pm 10$	3	0.83	0.75
3C 84	0.0172	59600	$1520 \pm 3$	$1300 \pm 300$	4	0.93	1.12
3C 192†	0.0598	8	$51 \pm 0.9$	$< 5$	1	0.44	$> 1.47$
3C 264	0.0208	200	$213 \pm 2$	$486 \pm 10$	5	0.60	0.96
3C 272.1	0.0031	180	$49 \pm 0.9$	$26 \pm 6$	1	0.72	1.20
3C 274	0.0043	4000	$679 \pm 2$	$1080 \pm 20$	1	0.79	1.00
3C 296	0.0237	77	$10 \pm 2$	$58 \pm 7$	1	0.78	0.83
3C 310	0.0540	80	$20 \pm 0.9$	$28 \pm 5$	1	0.73	1.04
3C 338	0.0298	105	$27 \pm 0.9$	$20 \pm 7$	1	0.73	1.16
NGC 6251	0.024	850	$186 \pm 2$	$370 \pm 20$	6	0.75	0.96
3C 382†	0.0578	188	$3180 \pm 6$	$5950 \pm 100$	1	0.35	0.99
3C 390.3†	0.0569	330	$1220 \pm 4$	$4300 \pm 100$	1	0.49	0.89
3C 442A	0.0263	2	$4 \pm 0.7$	$< 20$	1	0.55	$> 0.88$
3C 449	0.0171	37	$28 \pm 1$	$20 \pm 6$	1	0.63	1.19
3C 465	0.0293	270	$55 \pm 2$	$66 \pm 6$	1	0.75	1.06

Sources marked with a dagger are classed as FRIIs. Errors are  $1\sigma$  and are statistical only. We have not attempted to compute the errors in the optical data due to background subtraction uncertainties. X-ray data are taken from Hardcastle & Worrall (1999). Radio references are as follows: (1) Giovannini et al. (1988); (2) Leahy, Jägers & Pooley (1986); (3) O’Dea & Owen (1985); (4) Noordam & de Bruyn (1982); (5) Gavazzi, Perola & Jaffe (1981); (6) Jones et al. (1986).

**Figure 3.** Two-point radio-to-optical and optical-to-X-ray spectral indices


Boxes denote radio galaxies, and filled boxes are the broad-line radio galaxies. Arrows denote lower limits due to X-ray non-detections. Plotted with our data points are the BL Lacs from the sample of Fossati et al. (1998). Here filled triangles are radio-selected BL Lac objects from the 1-Jy sample and open triangles are X-ray selected BL Lacs from the Slew survey. The line indicates the locus of spectra that can be described as single power laws.

**Table 1.** Archival *HST* data for 3CRR radio galaxies with  $z < 0.06$ 

Source	Obs. status	Filter	Duration (s)
3C 31	OK	F702W	280
3C 33	Not observed		
3C 66B	OK	F702W	280
3C 76.1	Not observed		
3C 83.1B	Diffraction spike	F702W	280
3C 84	Saturated	F702W	560
3C 98	Mispointed		
DA 240	Not observed		
3C 192	WFC observations	F702W	280
4C 73.08	Not observed		
3C 264	OK	F702W	280
3C 272.1 (M84)	OK	F702W	280
3C 274 (M87)	OK	F814W	2430
3C 293	Disturbed	F702W	280
3C 296	OK	F702W	280
3C 305	Extended	F702W	560
3C 310	OK	F702W	280
NGC 6109	Not observed		
3C 338	OK	F702W	280
NGC 6251	OK	F814W	1000
3C 382	Saturated	F702W	280
3C 386	Foreground star	F702W	280
3C 390.3	Saturated	F702W	280
3C 442A	OK	F791W	750
3C 449	OK	F702W	280
NGC 7385	Not observed		
3C 465	OK	F702W	280

Notes: Sources with ‘saturated’ optical nuclei yield only a lower limit on their optical flux densities; 3C 382 is the worst affected by this effect. 3C 83.1B’s nucleus lies close to the diffraction spike from a bright foreground star, so the optical flux density is uncertain. 3C 192 was observed in the Wide Field Camera (WFC), so the nucleus is not well resolved from background emission. 3C 293 shows strong, irregular dust features, and it is not clear which component, if any, is the optical core. 3C 305’s ‘nucleus’ is extended and off-axis, and probably related to scattering from a more strongly obscured true nucleus, or affected by line contamination (Jackson et al. 1995). A foreground star lies directly on the line of sight to the nucleus of 3C 386 (Lynds 1971), preventing a measurement of its flux.